PROCEEDINGS

February 11-12, 1971

ALTA AVALANCHE LIBRARY

SNOW AND ICE

In Relation to Wildlife and Recreation

SYMPOSIUM

Iowa State University
Memorial Union
Ames, Iowa

Sponsoring Agencies:
Iowa Cooperative Wildlife Research Unit
Iowa State University
Bureau of Sport Fisheries and Wildlife
Region 3

PROCEEDINGS

of the

SNOW AND ICE IN RELATION TO WILDLIFE AND RECREATION

SYMPOSIUM

February 11-12, 1971

Memorial Union
Iowa State University, Ames

Edited by Arnold O. Haugen

Sponsoring Agencies:
Iowa Cooperative Wildlife Research Unit
Iowa State University
Bureau of Sport Fisheries and Wildlife, Region 3

Published by

Iowa Cooperative Wildlife Research Unit
Iowa State University Ames, Iowa

1971

CHARACTERISTICS OF SLAB AVALANCHES

RONALD I. PERLA, Avalanche Hazard Forecaster, Alta Avalanche Study Center, Wasatch National Forest, Alta, Utah

Abstract: A nomenclature is developed to describe the fracture patterns of a slab avalanche. Following the Varnes description of landslide markings, the key terms are: crown (upslope portion of the fracture line), toe (downslope portion of the fracture line), flanks (side portions of the fracture line), and the bed surface (base slide surface of slab). Detailed observations of snow properties and slope characteristics were made on 23 slabs which released at Alta, Utah, during Winter 1969-70. The bed surface inclination was found to vary between 30^{o} and 45^{o} with a strong peak occurrence at 38^{o}. The bed surface radius of curvature was on the order of 10^{3} meters. In the majority of cases, the fracture line geometry in the plane of the slab consisted of an arc-shaped crown in combination with a saw-toothed flank. Crystals formed by temperature gradient metamorphism were found beneath 65% of the bed surface. The mean density, temperature, and shear frame strength of the 23 crown profiles were respectively: 228 kg m^{-3}, $-5.8^{o}C$, and 1610 N m^{-2}. The strength at the bed surface tended to be 50% weaker than the strength measured just above the bed surface. The ratio of the strength of the bed surface to the load on the bed surface varied between 1.04 and 4.53.

Location and Climatology of Study Area

This study was performed in its entirety at Alta (el. 2700m, $40^{o}36'/110^{o}38'$), which is a small village in the Wasatch Mountains of northern Utah. The 3600-meter summits of the Wasatch rise abruptly as a wedge, running north to south above the Salt Lake Valley (el. 1350m). The acute orographic effect of this wedge snares large amounts of moisture from the prevailing westerly storms, and makes the Wasatch a precipitation anomaly in an otherwise relatively dry region. Table 1 shows the precipitation, temperature, and avalanche data of the Alta winters as averaged over the 25-year period, 1945-1970. The precipitation data are based on daily core samples and a total depth measurement, both taken at a level study plot (el. 2700m). The temperature data are based on maximum-minimum thermometers (el. 2700m). The slab avalanche observations of this study were compiled during the 1969-1970 winter. As also shown in Table 1, the climatology of 1969-1970 did not depart drastically from the 25-year averages.

Nomenclature for Slab Avalanches

The existing, informal nomenclature of slab avalanche components is too limited for the purposes of a quantitative study. Moreover, the current terms tensile zone, neutral zone, and compressive zone imply a priori knowledge of the complex stress distribution in the slab before failure. Although there are reasons to believe that the above zones exist, nonetheless, distinct stress zones are not observed directly; what is observed is the fracture pattern which remains on the slope after slab release, and which furnishes information on the stress distribution at failure and on

the origin of the instability. Therefore, a nomenclature based on fracture patterns has been developed to facilitate discussion of slab mechanics. This nomenclature was influenced somewhat by the Varnes (1958) description of landslide markings.

With reference to Fig. 1, a plan view of an idealized slope upon which is superimposed a typical fracture line, and Fig. 2, a view of the typical fracture surfaces remaining after slab release, the following nomenclature is specified.

Fracture line - On the snow-air surface, the closed curve which demarcates the boundary of the slab.

Crown line - The upslope section of the fracture line, usually an arc.

Toe line - The downslope section of the fracture line, often obliterated when bulldozed over by the falling slab.

Right and left flank lines - The side sections of the fracture line, usually jagged. In keeping with geological nomenclature, right and left refer to the slab as viewed downslope from the crown line.

Crown - The snowpack which is immediately upslope from the crown line.

Toe - The snowpack which is immedately downslope from the toe line.

Right and left flank - The snowpack which is respectively to the right and left of the right and left flank lines.

Correspondingly, the slab is also subdivided into: Slab crown, Slab toe, Slab right flank, Slab left flank, and Slab center. Furthermore, since fracture lines tend to reappear from season to season, or even from storm to storm, in almost the same slope position, it is reasonable, when the position of the fracture line is approximately predictable, to subdivide each slope into: crown region, central region, toe region, and flank regions.

The fracture line is the bounding curve of the fracture surface which can be subdivided into: crown surface, flank surfaces, and the bed surface. The latter comprises by far the greatest portion of the fracture surface.

The crown profile (Fig. 3a) consists of: snow-air surface, slab layer, bed surface extension, slab substratum, and ground surface. With reference to conditions before slab release, the crown region profile (Fig. 3b) consists of: snow-air surface, crown region layer, and ground surface. Similar terminology can be applied to the flank and toe regions. The slab layer, slab substratum, and crown region layer may each consist of several laminates, numbered consecutively; e.g., slab layer laminate 1, slab layer laminate 2, etc., with the higher number laminates closer to the ground surface. Within the crown region layer, potential bed surfaces may be associated with weak laminates or the discontinuity between adjacent laminates.

Method of Slab Observation and Measurement

Observations of fracture geometry and snow properties were made at 23 fracture lines on the average of a few hours after slab release. In two instances, the author equipped with field instrumentation ski-released a small slab and was afforded the opportunity of immediate measurement. However, the majority of the measurements were made on large slabs which were released by explosives or artillery, and to which access was not possible until safe approach routes could be established. The maximum delay between slab release and fracture line observation was about 24 hours. Large delays were permitted only on north facing slopes where reduced radiation would not drastically alter the snow properties during the delay. Measurement of south-facing fracture lines was all completed within a few hours after slab release. Observations were not taken after mid-March since the intense solar radiation of spring quickly metamorphoses the snow on all exposures and measurements taken even a few hours after slab release would not represent conditions at time of release.

Although it would have been preferable to measure snow properties at several points along the fracture line, there was insufficient time for the author, working alone, to take readings at more than one fracture location. The approximate center of the crown line was chosen as the standard observation location because the crown line was the least disturbed and most easily identified section of the fracture line.

Accessibility to the crown line was usually a problem since a general hazard existed just when conditions were most interesting. Careful route-finding and other precautions of winter mountaineering were required. Equipment management at the crown line was troublesome since the bed surface was usually steep and smooth. One slip would have sent equipment and observer on a devastating ride.

The entire crown profile, with special emphasis on the bed surface extension, was sampled in a 1m x 1m slot which was shoveled out of the crown. In this slot, the author, working downward from the snow-air surface, measured at about 8 cm intervals the density, temperature, crystal structure, and shear frame strength of the snow. Density was measured by a Swiss portable density kit, temperature by a dial thermometer, crystal structure by a 10x hand lens, and snow strength by a shear frame (Roch 1966a,b).

Before leaving the crown line, the crown surface was examined for fracture markings, the shape of the fracture line with relation to surface protrusions was sketched, and the angle between the crown surface and the bed surface, averaged over the entire crown line, was judged with the aid of a rectangular plate as falling into one of the categories: greater than, less than, or equal to 90^{o}.

After completion of the crown line observations, a pit was dug at the approximate center of the bed surface and the crystal structure of the slab substratum was noted. Finally, the mean inclination of the bed surface to the horizontal was measured to the nearest degree with an inclinometer, and the curvature of the bed surface was judged as either convex, imperceptible, or concave.

Summary of Slab Observations

Table 2 summarizes the Alta slab observations for the season 1969-70. As shown in Column 4, the vast majority of the investigated slabs were triggered artificially by either artillery, hand-thrown explosives, or ski tracks. In two cases, Slab Nos. 3 and 11, a primary avalanche released by artillery caused the release of a secondary avalanche. A falling cornice, kicked loose by a skier, triggered Slab No. 16. The trigger for Slab No. 15 was unknown.

Over the Wasatch Range, the prevailing winds are westerlies which tend to snow load east facing slopes more frequently than other exposures. As shown in Table 1, Column 5, the majority of the investigated slabs face east; however, all points of the compass are represented. The slabs were contained in a relatively narrow band of elevation, between 3100m and 3500m above sea level, and within a horizontal area of about 3 km^2.

Based on the remaining columns of data and information from other investigations, the empirical features of slab avalanches are as follows:

A. Bed surface inclination. Table 3 summarizes the data of five international investigations on slab occurrence versus bed surface inclination. The data of these investigations are plotted in Fig. 4 where it is clearly seen that the bed surface inclination, with rare exception, is between 30^0 and 45^0, and has a strong peak at about 38^0.

B. Bed surface radius. Although the data of Table 2, Column 7, show that concave bed surfaces are predominant (i.e., the center of curvature is predominantly in the atmosphere), in almost all cases the radius of curvature was extremely large in comparison to the thickness of the slab layer (Table 2, Column 13); a typical radius of curvature (Slab No. 7, West Rustler) was determined approximately as

$$\frac{\text{length of bed surface}}{\text{inclination change}} = \frac{50 \text{ meters}}{3 \text{ degrees}} = 10^3 \text{ meters}$$

C. Crown and flank line geometry. From Table 2, Columns 8 and 9, it is evident that 75% of the fracture lines consist of an arc-shaped crown in combination with a saw-toothed flank. In about 50% of the cases, the arc appeared, under close observation, to be a smooth trajectory. The 23 observations of Table 2, in addition to 3 years of informal observation (1966-69) at Alta, did not support the Haefeli (1963) observation of a saw-toothed crown line.

Working with photographs of crown surfaces, Sommerfeld (1969) identified markings which resembled the microscopic markings found on the fracture surfaces of glass samples: mirror, mist, and hackle markings. Field examination of Alta crown surfaces could not verify the existence of such markings.

D. Crown surface-bed surface angle. While soil bodies exhibit two distinct modes of failure (Varnes 1958), rotational mode and block glide mode (Fig. 5), snow slabs fail exclusively by the block glide mode wherein the crown surface and the bed surface form two distinct planes which intersect at approximately

90^{o}. Although the bed surface is essentially planar, a precise value of the crown surface-bed surface angle is difficult to measure because the inclination of the crown surface meanders considerably. As shown in Table 2, Column 10, the angle tends to be greater than 90^{o}, but in all cases the deviation from 90^{o} was slight, and never more than 20^{o}.

E. Slab substratum. With reference to the classification system of Sommerfeld and LaChapelle (1970), wherein metamorphosed snow prior to firnification is classified as either equi-temperature metamorphosed (ET) or temperature gradient metamorphosed (TG), it was found (Table 2, Column 11) that in 65% of the investigated cases the slab substratum consisted of TG laminates. Mature depth hoar, i.e., complete TG metamorphism, was identified in Slab Nos. 14, 15, and 20.

F. Ratios: slab width-thickness and slab width-length. If we assume an arc-shaped crown then we may estimate the slab-width, which we define as the mean distance separating the right and left flank lines, as $2/\pi$ times the crown line length; whereupon from Table 2, Column 12, the mean ratio slab width/slab thickness is approximately 60. Similarly, Jaccard (1966) studied slabs which were half the width and half the thickness of the Alta slabs, but also concluded that the width/thickness ratio would be greater than 50.

The slab length which we define as the mean distance separating the crown line and the toe line is difficult to measure because, as indicated earlier, the toe line is usually obscured by the falling snow. Numerous informal observations during 1945-1970 suggest that the average slab width and average slab length are of similar dimensions, although the slab/length ratio for a specific case is highly dependent on the terrain. Frequently, the crown lines of individual adjacent slabs, which usually run independent of one another, interconnect over the entire mountainside so that the width/length ratio of the system of slabs is relatively large, perhaps on the order of 10. In other cases, the flank lines extend a considerable distance down gullies so that the width/length ratio is relatively small.

G. Properties of the slab layer. In one sense, the complexity of slab avalanche investigations is due to the wide variety of unstable slab layers, each unique in density, temperature, strength, and crystal form. On the other hand, the majority of slab layers exhibit certain general patterns: an increase in density with depth below the slab-air surface, an increase in temperature with depth, and relatively large scatter in the shear frame index. As an example, the properties of the West Rustler slab layer (Table 2, Slab No. 7) are plotted in Fig. 6.

From Table 2, the averaged properties of the investigated slabs are:

Mean thickness (average of Column 13)	0.94 m
Mean density (average of Column 14)	228 kg m^{-3}
Maximum density (average of Column 15)	285 kg m^{-3}
Minimum density (average of Column 16)	155 kg m^{-3}
Mean temperature (average of Column 17)	$-5.8^{o}C$

Maximum temperature (average of Column 18)----------	-4.1°C
Minimum temperature (average of Column 19)----------	-7.5°C
Mean shear frame index (average of Column 20)----------	1610 N m^{-2}
Maximum shear frame index (average of Column 21)----------	3306 N m^{-2}
Minimum shear frame index (average of Column 22)----------	537 N m^{-2}

The inhomogeneity of shear frame index is quite striking as is seen by forming the ratio maximum shear frame index (Column 21) to minimum shear frame index (Column 22) for each slab, and then averaging this ratio over all the cases to give

$$\frac{(\text{maximum shear frame index})}{(\text{minimum shear frame index})} = 7.34 \text{ average}$$

The density inhomogeneity, calculated in a similar manner, is also significant

$$\frac{(\text{maximum density})}{(\text{minimum density})} = 1.9 \text{ average}$$

H. Properties of the bed surface extension. First, it must be emphasized that in about 50% of the investigated slabs the bed surface extension was not found to be a well defined surface of discontinuity between adjacent laminates, but rather an extension of the bed surface into a relatively thick laminate. Although the bed surface extension could not always be located visually as a distinct surface, a significant variation between the shear frame index measured at the bed surface extension (Table 2, Column 23) and the shear frame index measured about 5 cm above the bed surface (Table 2, Column 24) was found:

$$\frac{\text{shear frame index 5 cm above bed surface extension}}{\text{shear frame index at bed surface extension}} = 1.5$$

From Column 25 we find the mean temperature of the bed surface extension to be -4.2°C. Finally, from Column 26 we note that the bed surface extension consists of a wide variety of crystal types. (For explanation of the crystal types, see: Sommerfeld and LaChapelle 1970; Magona and Lee 1966.) As we have argued in a recent paper (Perla and LaChapelle 1970), the properties of the bed surface (and its extension) are vital data for snow slab analysis.

The Strength-Load Ratio for the Bed Surface

Various strength-load ratios for the bed surface which are of the form

$$\frac{(\text{some strength index of the bed surface})}{(\text{some measurement related to the stress on the bed surface})}$$

have been proposed as practical quantitative aids in slab stability analysis. The proponents of the strength-load ratio technique, for example Krasnosel'skii (1964), Bradley (1970), and Gardner and Judson (1970), each recommend for the snowpack of their mountain range, a critical strength-load ratio, which is not necessarily unity, and which varies greatly depending on the type of strength and stress measurements employed. From a combined theoretical and

experimental standpoint, the most intricate study on strength-load ratios is due to Roch (1966a, 1966b) who chose a Coulomb-Mohr strength criterion for the biaxial behavior of snow, and performed his strength and stress measurements on the bed surface extension of actual slabs, in contrast to Krasnosel'skii, Bradley, and Gardner and Judson who developed correlations between the general avalanche activity in their respective mountain ranges and data either gathered from level study plots or from slopes which may or may not have avalanched.

First, Roch (1966a) determined the Coulomb-Mohr characteristics of alpine snow by placing weights of various magnitudes on his shear frame, and thus measured the effect of normal stress σ_N on the shear frame index τ_s. He found that his data fit the expression

$$\tau_s = C + (0.4 + 0.00008\ C)\ \sigma_N \qquad (1)$$

where τ_s, C, and σ_N are in Nm^{-2}, and C is the cohesion of the snow, that is, the shear frame index for $\sigma_N = 0$. Next, Roch (1966b) toured to the fracture line of 36 slabs and measured the cohesion (C) of the bed surface extension, the density throughout the slab layer (ρ), and the bed surface inclination (θ). On the assumption that the shear stress acting on the bed surface is given by

$$\sigma_t = g \sin\theta \int_{\text{bed surface}}^{\text{snow-air surface}} \rho(y)\,dy \qquad (2)$$

and the normal stress acting on the bed surface is given by

$$\sigma_N = g \cos\theta \int_{\text{bed surface}}^{\text{snow-air surface}} \rho(y)\,dy \qquad (3)$$

he calculated for his 36 cases the strength-load ratio τ_s/σ_t, and found

i. Range of τ_s/σ_t ..... 0.76 - 7.50

ii. Average of τ_s/σ_t 2.05

iii. 97.5% of the cases ..... $\tau_s/\sigma_t < 4.0$

92.0% of the cases ..... $\tau_s/\sigma_t < 3.5$

86.5% of the cases ..... $\tau_s/\sigma_t < 3.0$

Similarly, Table 4 shows the strength-load data for the 23 Alta slabs of Table 2. Roch's method of calculating τ_s/σ_t was followed. τ_s was calculated from (1) wherein C is taken from Table 2, Column 23, σ_t from (2), and σ_n from (3). From the Alta data we find:

i. Range of τ_s/σ_t ..... 1.04 - 4.53

ii. Average of τ_s/σ_t 2.41

iii. 95.5% of the cases ..... $\tau_s/\sigma_t < 4.0$

95.5% of the cases ..... $\tau_s/\sigma_t < 3.5$

81.7% of the cases ..... $\tau_s/\sigma_t < 3.0$

Conclusions

The averaged properties of the 23 investigated slabs must reflect the climatological pecularities of Alta. For the purpose of avalanche hazard evaluation, it would be interesting if comparisons of slab data could be established between different climate zones (at present, data similar to Table 2, Columns 13-22, are not reported elsewhere in the literature) so that slab properties which are determined by the specific climatology of an area can be separated from properties intrinsic to the avalanche phenomena.

The simplest explanation for the nearly perpendicular angle between the crown surface and the bed surface is that failure commences along the bed surface and propagates into the crown surface. This leads to the interesting conclusion that explosives for avalanche control will be more effective if placed near the slab center instead of in the crown region.

Since the bed surface was found to be distinctly weak in comparison to the laminate immediately above the bed surface, there appears to be some practical merit in strength testing of the snowpack for avalanche hazard evaluation. On the other hand, the wide variation in the strength-to load ratios observed by both the author (Table 4) and Roch (1966b) seems to indicate the unreliability of these ratios in avalanche forecasting.

Acknowledgment

Encouragement and guidance given to the author by Dr. E. R. LaChapelle is gratefully acknowledged.

Literature Cited

Bader, H. et al. 1939. Der Schnee und seine Metamorphose, von H. Bader, R. Haefeli, E. Bucher, J. Neher, O. Eckel, C. Thams, P. Niggli. Beiträge zur Geologie der Schweiz. Geotechnische Serie. Hydrologie, Lief. 3. [English translation: U.S. Snow, Ice and Permafrost Research Establishment. Translation 14, 1954.]

Bradley, C. C. 1970. The location and timing of deep slab avalanches. J. Glaciology 9(56):253-261.

Gardner, N. C. and A. Judson. 1970. Artillery control of avalanches along mountain highways. USDA Forest Serv. Rocky Mountain Forest and Range Expt. Sta. Ft. Collins, Colo. Res. Paper RM-61.

Haefeli, R. 1963. Stress transformations, tensile strengths and rupture processes of the snow cover. (In Kingery, W. D., ed. Ice and snow; properties, processes, and applications: proceedings of a conference held at Mass. Inst. Technol. Feb. 12-16, 1962. Cambridge, Mass. The M.I.T. Press. 560-575.)

Jaccard, C. 1966. Stabilité des plaques de neige. Union de Géodésie et Géophysique Internationale. Assoc. Internationale d'Hydrologie Scientifique. Commission pour la Neige et la Glace. Div. Neige Saisonnière et Avalanches. Symposium international sur les aspects scientifiques des avalanches de neige, 5-10 avril 1965, Davos, Swisse, 170-181.

Krasnosel'skiĭ, E. B. 1964. K voprosu opredeleniia stepeni lavinnoĭ opasnosti v vysokogornykh raĭonakh tsentral'nogo Tian' - Shania. [Determining the degree of avalanche danger in the high mountain regions of central Tien Shan.] Leningrad. Glavnaia Geofizicheskaia Observatoriia, Trudy, No. 150. 133-139.

Magono, C. and C. W. Lee. 1966. Meteorological classification of natural snow crystals. J. Faculty of Sci. Hokkaido Univ. Ser. 7, 2(4):321-335.

Perla, R. and E. Lachapelle. 1970. A theory of snow slab failure. J. Geophysical Res. (in press).

Roch, A. 1966a. Les variations de la résistance de la neige. Union de Géodésie et Géophysique Internationale. Assoc. Intern. d'Hydrologie Sci. Comm. pour la Neige et la Glace. Div. Neige Saisonnière et Avalanches. Symposium intern. sur les aspects scientifiques des de neige, 5-10 avril 1965, Davos, Swisse. 86-99.

_____. 1966b. Les declenchements d'avalanches. Union de Géodésie et Géophysique Internale. Assoc. Intern. d'Hydrologie Sci. Comm. pour la Neige et la Glace. Div. Neige Saisonnière et Avalanches. Symposium intern. sur les aspects scientifiques des avalanches de neige, 5-10 avril 1965, Davos, Swisse, 182-195.

Sommerfeld, R. A. 1969. The role of stress concentration in slab avalanche release. J. Glaciology 8(54):451-462.

_____and E. LaChapelle. 1970. The classification of snow metamorphism. J. Glaciology 9(55):3-17.

Varnes, D. J. 1958. Landslide types and processes. (In Eckel, E. B., ed. Landslides and engineering practice: Highway Res. Bd. Spec. Rept. No. 29. Washington, D.C. 20-47).

Wakabayashi, R. and M. Yamamura. 1968. Features of snow slab avalanches in Hokkaido. Japanese Soc. Snow and Ice. Tokyo. J.(Seppyo). 30(3):75-80.

Table 1. Climatology, Alta, Utah, 1945-1970, 1969-1970.

	Snow-fall (cm)	Water content (cm)	Maximum snow depth on ground (cm)	Number days with 30 cm or more of new snow	Ava-lanche days	Mean daily maximum °C	Mean daily minimum °C
			Mean data for 1945 - 1970				
Dec.	224	20.6	153	2.16	8.14	+0.3	- 9.5
Jan.	232	22.2	226	2.12	10.34	-1.1	-11.0
Feb.	200	18.2	266	2.00	9.04	-0.4	-10.3
Mar.	214	20.2	306	1.92	10.49	+0.4	- 9.5
Total	870	81.2	---	8.20	38.01	---	--
			Mean data for 1969 - 1970				
Dec.	178	13.4	132	1	11	+0.5	- 8.7
Jan.	263	30.0	256	2	13	-3.3	-10.4
Feb.	154	14.0	272	1	4	+1.1	- 8.5
Mar.	198	18.3	292	1	10	-1.8	-10.8
Total	793	75.7	---	5	38	---	--

Table 2. Slab observations, Alta, Utah, 1969-70.

Slab No.	Name	Date	Trigger	Aspect	Bed surface inclination degree	Bed surface radius	Crown line geom.	Flank line geom.	Crown-bed angle	Slab substratum	Crown line length (m)	Slab thickness (m)
1	2	3	4	5	6	7	8	9	10	11	12	13
1	Baldy Face	12/22/69	Artillery	N	33	Concave	Arc	Tooth	1	T.G	50	0.50
2	Baldy Chute E.	"	"	NE	35	"	"	Arc	More	E.T	80	0.30
3	Baldy Chute E.	"		NE	35	"	"	"	"	T.G	80	0.85
4	Upper Peruvian Ridge	"	Hand explosives	E	36	Convex	"	Tooth	"	T.G	60	0.70
5	E. Greeley Chute	12/25/69	Artillery	E	40	Concave	"	"	1	T.G.	60	0.65
6	Upper Peruvian Ridge	"	Hand explosives	E	35	Convex	"	"	1	T.G	60	0.80
7	W. Rustler	12/27/69	"	W	40	Concave	"	"	More	T.G	40	1.00
8	Stone Crusher	"	Artillery	NW	40	"	"	"	1	T.G	40	0.90
9	Sunspot	12/29/69	Skier	W	39	∞	"	"	More	T.G	70	0.60
10	Flagstaff Shoulder	1/18/70	Artillery	S	33	Convex	"	"	1	T.G	100	0.77
11	Flagstaff Shoulder	"	10	SE	34	"	"	Arc	More	T.G	80	1.36
12	Cardiff	"	Artillery	SE	38	Concave	"	"	"	E.T	400	1.43
13	Flagstaff Mtn.	1/22/70	"	S	35	∞	"	Tooth	"	T.G	100	1.08
14	Jitterbug	"	"	W	42	Concave	"	"	1	T.G	40	1.60
15	Race Course	1/24/70	?	NW	36	∞	"	"	Less	T.G.	100	1.30
16	Yellow Trail	1/25/70	Cornice	E	40	∞	Tooth	"	More	E.T.	50	0.91
17	E. Greeley	"	Artillery	E	38	Concave	Arc	"	?	E.T.	100	4.20
18	Lower Peruvian Ridge	1/30/70	Skier	E	47	"	Tooth	"	Less	E.T	40	0.80
19	Gunsight	2/20/70	"	E	40	Convex	Arc	"	"	E.T	25	0.50
20	Secret Lake	3/6/70	"	N	35	∞	"	"	1	T.G	70	0.49
21	Jitterbug	3/9/70	"	W	40	Concave	"	"	More	E.T	15	0.18
22	Lone Pine	"	"	N	42	"	"	"	1	E.T.	10	0.18
23	Flagstaff Shoulder	3/18/70	Artillery	SE	38	"	"	"	More	E.T	100	0.48

Table 2. Continued

Slab No,	Density ($kg\ m^{-3}$) Mean	Max.	Min.	Temperature (^{o}C) Mean	Max.	Min.	Shear frame index (Nm^{-2}) Mean	Max.	Min.	Sh.fr. ind. at bed surface Nm^{-2}	Sh.fr.ind. above bed surface Nm^{-2}	Temperature ^{o}C	Crystal form
1	14	15	16	17	18	19	20	21	22	23	24	25	26
1	260	300	200	-8	-5	-14	1350	2400	500	1600	2400	-5	E.T
2	250	300	200	-7	-5	- 8	1770	3000	300	950	2600	-5	(a)
3	240	290	170	-8	-6	- 9	2600	3300	2400	1100	2400	-6	E.T
4	250	280	200	-5	-2	- 9	1800	2700	100	1200	2400	-1	E.T
5	230	280	160	-5	-3	- 6	3000	9500	150	2200	1800	-2	T.G
6	220	280	140	-3	-2	- 5	1600	2300	300	1400	2300	-2	T.G
7	240	310	140	-4	-1	- 6	1660	3200	60	1900	2200	-1	T.G
8	210	320	100	-5	-3	- 7	2200	3400	800	2000	2600	-3	T.G
9	220	260	100	-9	-3	-13	1980	4000	300	2800	4000	-3	E.T.
10	250	340	120	-1	0	- 3	2380	4000	300	2600	4000	-1	T.G
11	260	360	140	?	?	?	?	?	?	2800	?	?	T.G.
12	240	320	160	-5	-5	- 4	2220	4200	450	3300	3600	-5	E.T
13	240	310	160	-2	-1	- 2	2180	3460	900	2900	3500	-1	T.G
14	300	400	240	-2	-1	- 3	4000	10000	1460	1500	2300	-1	T.G
15	250	300	180	-4	-4	- 5	2300	3820	800	1400	1900	-3	T.G
16	370	420	350	-5	-5	- 7	?	?	?	2900	?	-5	E.T
17	350	400	?	?	?	?	?	?	?	7300	?	-5	E.T
18	170	230	84	-9	-5	-13	1220	2300	140	1900	1700	-5	E.T
19	230	250	184	-12	-12	-12	840	1000	600	600	600	-13	E.T
20	140	180	96	-9	-6	-10	990	2000	400	1000	2000	-10	(b)
21	110	110	110	-9	-9	-10	290	300	280	200	300	- 7	(c)
22	90	100	80	-6	-5	- 7	220	240	200	200	200	- 5	(c)
23	140	210	94	-4	-4	- 5	600	1000	300	800	1000	- 3	(d)

Legend:

∞ ----imperceptible curvature
1 ----about 90
less ----slightly less than 90
more ----slightly more than 90

T.G ---Temperature gradient crystals
E.T ---Equi-temperature crystals
(a) ---Graupe
(b) ---Surface hoar

(c)---Rime free dendrites over a hard crust
(d)---Equi-temperature crystals over a hard crust

Table 3. Observed bed surface inclinations.

Investigation	Location	Number cases	Range of slope (degrees)	Average (degrees)
Perla (Table 1, Col. 6)	Alta	23	33-47	38
Haefeli (Bader, 1939)	Switzerland	5	33-40	36
Wakabayashi and Yamamura (1968)	Japan	5	33-40	34
Roch (1966b)	Switzerland	36	30-55	40
LaChapelle (personal communications of Alta data, 1964)	Alta	30	33-46	38

Table 4. Strength-load data, Alta, Utah

Slab No. (Table 2)	σ_t Nm^{-2}	σ_n Nm^{-2}	C Nm^{-2}	τ_s Nm^{-2}	τ_s / σ_t
1	860	1333	1600	2305	2.68
2	430	613	950	1242	2.89
3	1120	1600	1100	1880	1.68
4	1100	1510	1200	1950	1.77
5	880	1050	2200	2805	3.19
6	735	1050	1400	1936	2.64
7	1430	1700	1900	2840	1.99
8	1250	1480	2200	2829	2.26
9	745	920	2800	3374	4.53
10	1040	1600	2600	3571	3.43
11	2010	2980	2800	4660	2.32
12	2080	2660	3300	5330	2.56
13	1480	2100	2900	4230	2.86
14	3220	3580	1500	3360	1.04
15	1900	2610	1400	2740	1.44
16	2200	2610	2900	4550	2.07
17	-	-	-	-	-
18	908	850	1900	2368	2.61
19	708	840	600	977	1.37
20	396	566	1000	1272	3.21
21	124	147	200	261	2.11
22	112	125	200	252	2.25
23	460	585	800	1072	2.33

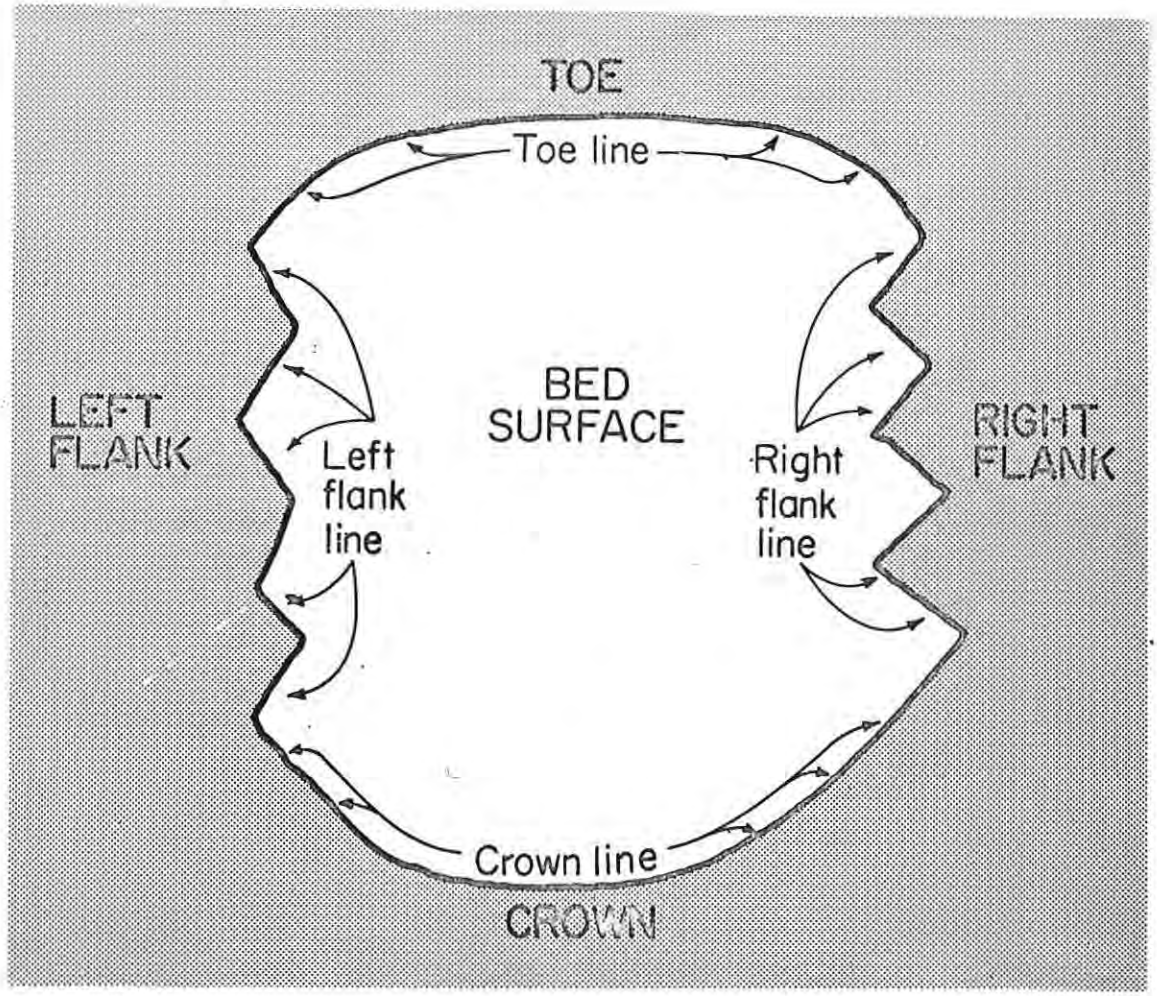

Fig. 1. Plan view of fracture line.

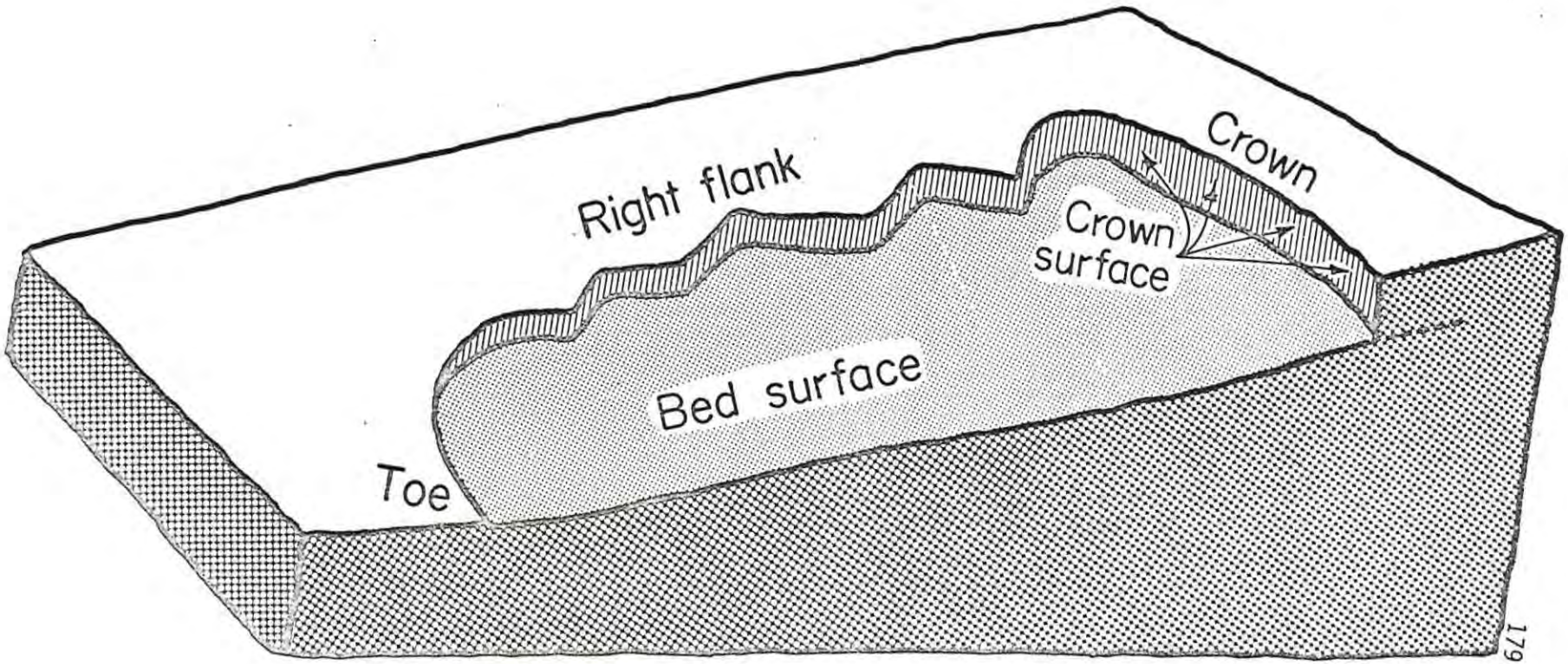

Fig. 2. Typical fracture surfaces remaining after slab release.

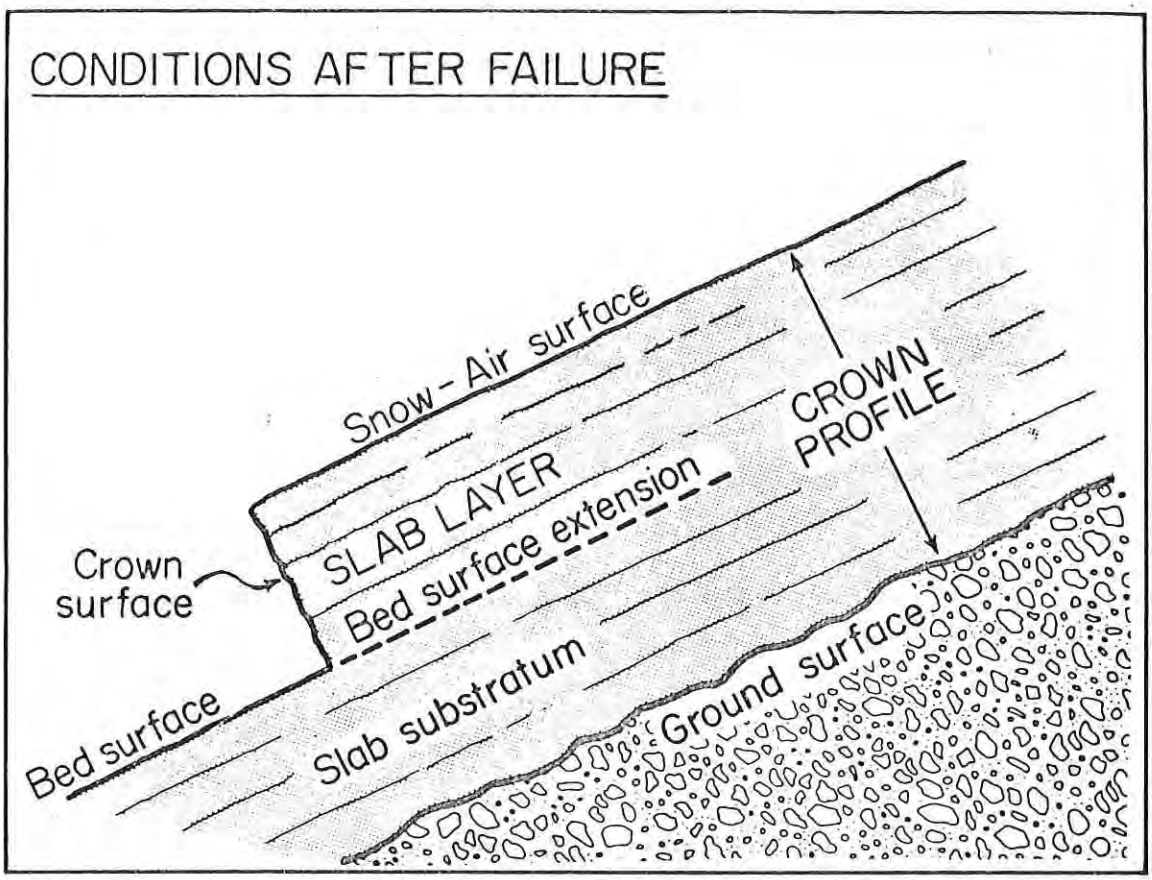

Fig. 3a. The crown profile.

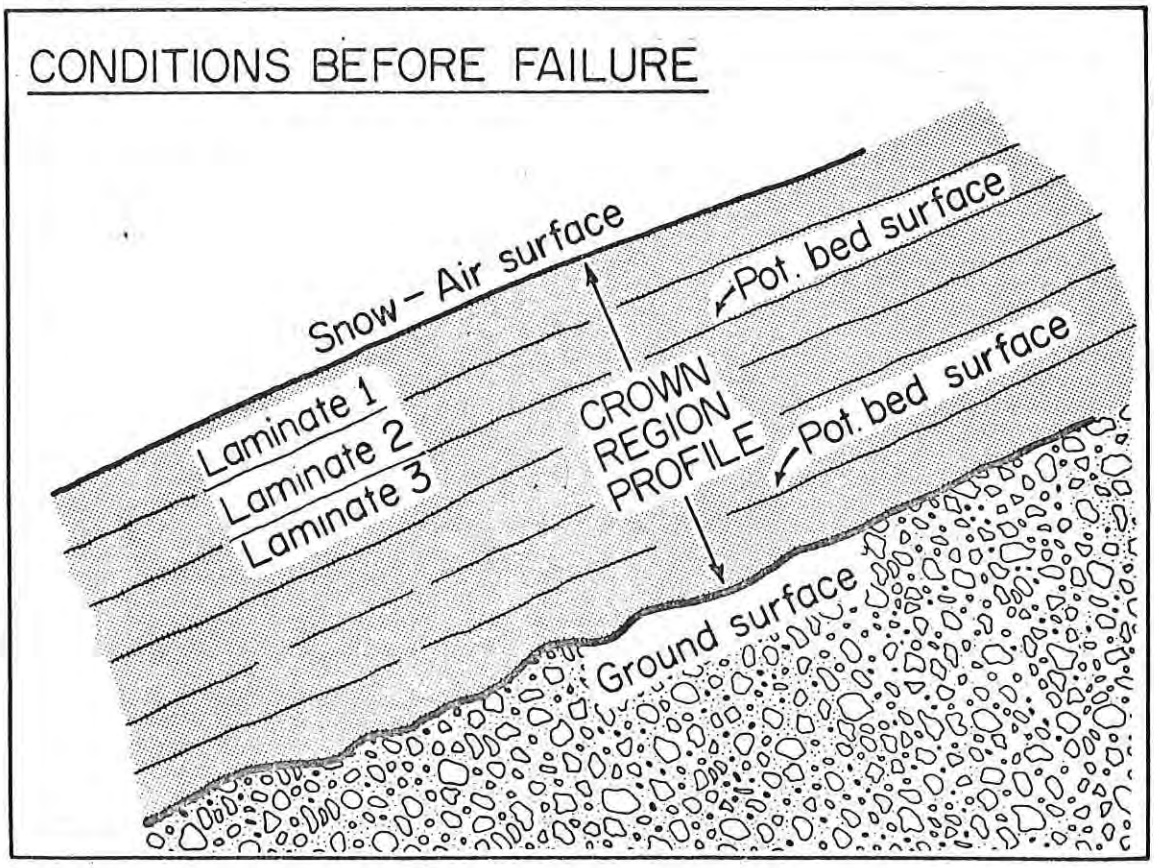

Fig. 3b. The crown region profile.

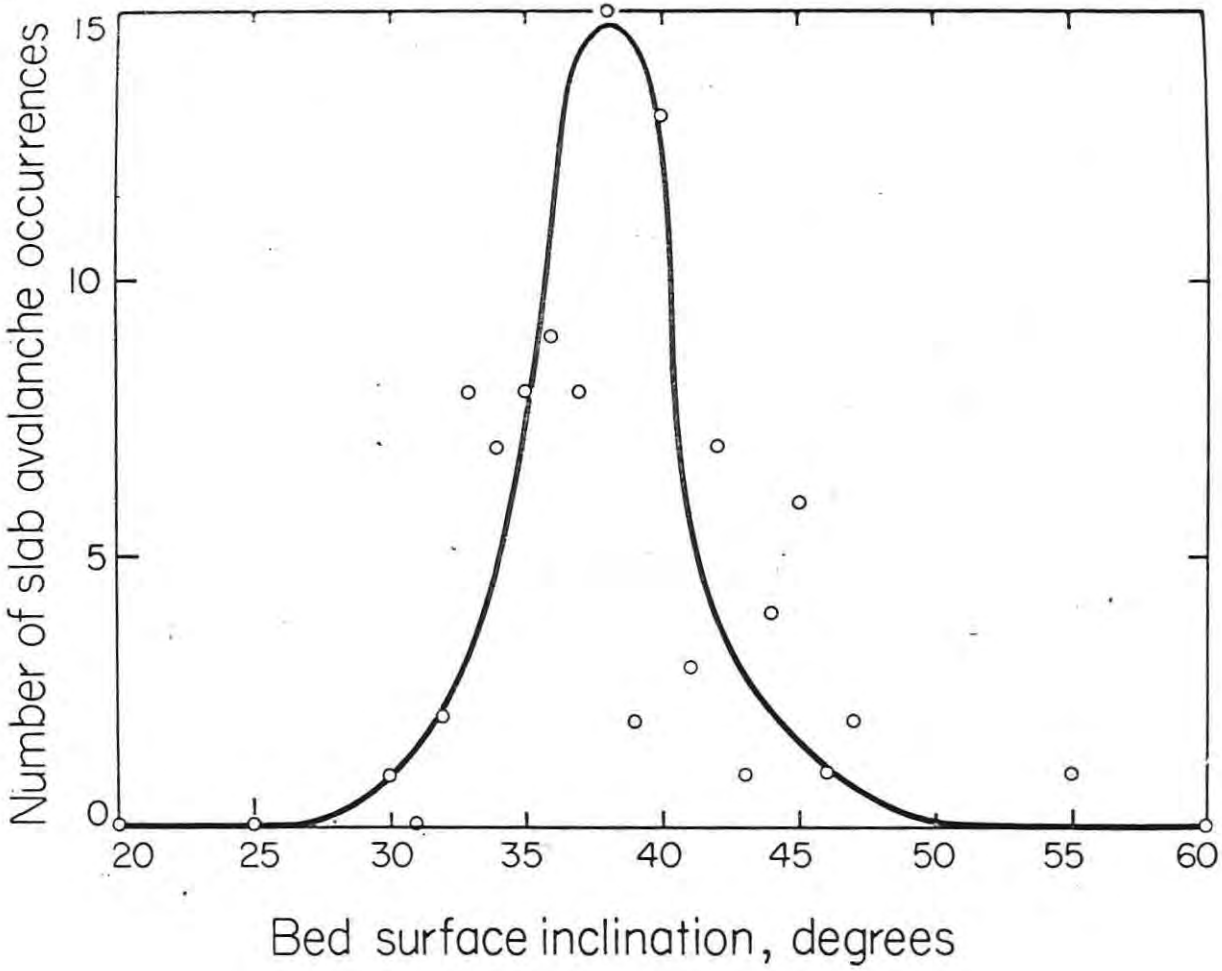

Fig. 4. Slab occurrences versus bed surface inclination.

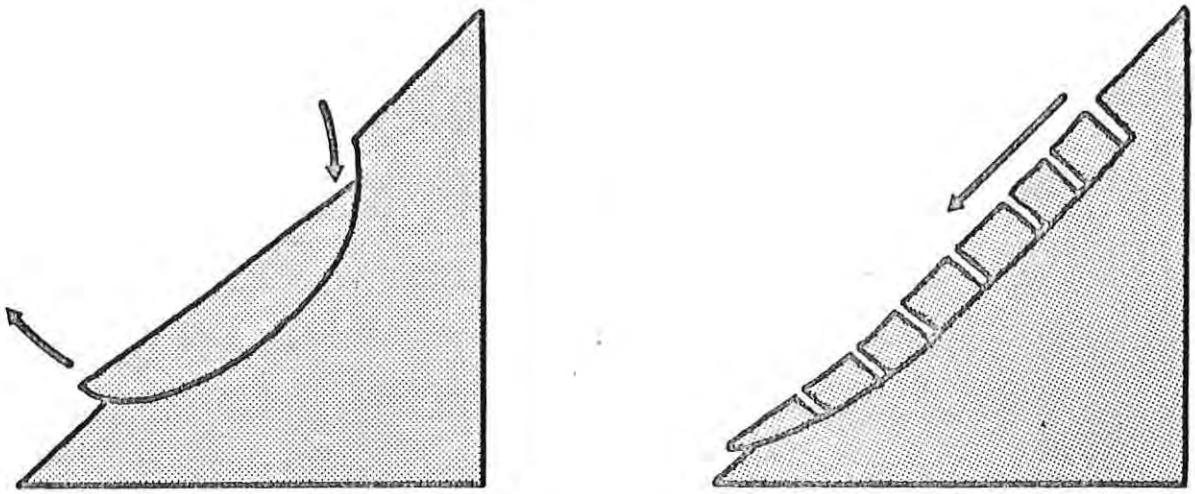

Fig. 5. Two modes of failure exhibited by soil bodies.